Transport in Porous Media **43:** 537–555, 2001.

Water Injection into a Low-Permeability Rock - 1: Hydrofracture Growth

TAD W. PATZEK[1,2] and DMITRIY B. SILIN[1]
[1]*Lawrence Berkeley National Laboratory, 1 Cyclotron Rd, MS 90-1116, Berkeley, CA 94720, U.S.A.*
[2]*University of California, Berkeley, Materials Science and Mineral Engineering, 591 Evans Hall, Berkeley, CA 94720-1760, U.S.A.*

(Received: 30 June 1999; in final form: 16 Aug 2000)

Abstract. In this paper, we model water injection through a growing vertical hydrofracture penetrating a low-permeability reservoir. The results are useful in oilfield waterflood applications and in liquid waste disposal through reinjection. Using Duhamel's principle, we extend the Gordeyev and Entov (1997) self-similar 2D solution of pressure diffusion from a growing fracture to the case of variable injection pressure. The flow of water injected into a low-permeability rock is almost perpendicular to the fracture for a time sufficiently long to be of practical interest. We revisit Carter's model of 1D fluid injection (Howard and Fast, 1957) and extend it to the case of variable injection pressure. We express the cumulative injection through the injection pressure and effective fracture area. Maintaining fluid injection above a reasonable minimal value leads inevitably to fracture growth regardless of the injector design and the injection policy. The average rate of fracture growth can be predicted from early injection. A smart injection controller that can prevent rapid fracture growth is needed.

Key words: optimal control, hydrofracture growth, waterflood, transient flow, generalized Carter model, self-similar solution.

Nomenclature

A	fracture area, m^2.
k	absolute rock permeability, md, $1\,\text{md} \approx 9.87 \times 10^{-16}\,m^2$.
k_{rw}	relative permeability of water.
p_i	initial pressure in the formation outside the fracture, Pa.
p_{inj}	injection pressure, Pa.
q	injection rate, l/Day.
Q	cumulative injection, l.
v	superficial leak-off velocity, m/Day.
w	fracture width, m.
α_w	hydraulic diffusivity, m^2/Day.
μ	viscosity, cp.
ϕ	porosity.
φ, θ	dimensionless elliptic coordinates.

1. Introduction

In this paper, we model water injection through a horizontally growing vertical hydrofracture totally penetrating a horizontal, homogeneous, isotropic and low-permeability reservoir initially at constant pressure. More specifically, we consider the soft diatomaceous rock with roughly a tenth of millidarcy permeability. Diatomaceous reservoirs are finely layered and each major layer is usually homogeneous, see (Zwahlen and Patzek, 1997a; Patzek and Silin, 1998) over a distance of tens of meters.

Our long-term goal is to design a field-wide integrated system of waterflood surveillance and control. Such a system consists of Waterflood Analyzer (De and Patzek, 1999) software integrated with a network of individual injector controllers. This paper focuses on the design of the injection controller; in the first part we develop the controller model, which is used in the second part to design several optimal controllers.

We consider the process of hydrofracture growth on a large time interval; therefore, we assume that at each time the injection pressure is uniform inside the fracture. We use modeling to relate the cumulative fluid injection and the injection pressure. To obtain the hydrofracture area, however, we rely either on independent measurements or on an analysis of injection rate – injection pressure data via inversion of the controller model. We do not yet rely on the various fracture growth models because they are insufficient. Instead, we analyze the mass of injected fluid and determine the fracture status juxtaposing the injected liquid volume with the leak-off rate at a given fracture surface area. The inversion of the model provides an effective fracture area, rather than its geometric dimensions. However, it is exactly the parameter needed as an input to the controller. After calibration, the inversion produces the desired input at no additional cost.

Patzek and Silin (1998) have analyzed 17 waterflood injectors in the Middle Belridge diatomite (CA, USA), three steam injectors in the South Belridge diatomite, as well as 44 injectors in a Lost Hills diatomite waterflood. The field data show that the injection hydrofractures grow with time. An injection rate or pressure that is too high may dramatically increase the fracture growth rate and eventually leads to a catastrophic fracture extension and unrecoverable water channeling between an injector and a producer. In order to avoid fatal reservoir damage, smart injection controllers should be deployed.

Field demonstrations of hydrofracture propagation and geometry are scarce, Kuo *et al.* (1984) proposed a fracture extension mechanism to explain daily wellhead injection pressure behavior observed in the Stomatito Field A fault block in the Talara Area of the Northwest Peru. They have quantified the periodic increases in injection pressure, followed by abrupt decreases, in terms of Carter's theory (Howard and Fast, 1957) of hydrofracture extension. Patzek (1992) described several examples of injector-producer hydrofracture linkage in the South Belridge diatomite, CA, and quantified the discrete extensions of injection hydrofractures using the linear transient flow theory and linear superposition method.

Vinegar et al. (1992) used three remote 'listening' wells with multiple cemented geophones to triangulate the microseismic events during the hydrofracturing of a well in a steam drive pilot in Section 29 of the South Belridge diatomite. Ilderton *et al.* (1996) used the same geophone array to triangulate microseismicity during hydrofracturing of two steam injectors nearby. In addition, they corrected the triangulation for azimuthal heterogeneity of the rock by using conical waves. Multiple fractured intervals, each with very different lengths of hydrofracture wings, as well as an unsymmetrical hydrofracture, have been reported. An up-to-date overview of hydrofracture diagnostics methods has been presented in Warpinski (1996).

To date, perhaps the most complete images of hydrofracture shape and growth rate *in situ* have been presented by Kovscek *et al.* (1996a,b). They have obtained detailed time-lapse images of two injection hydrofractures in the South Belridge diatomite, Section 29, Phase II steam drive pilot. Using a simplified finite element flow simulator, Kovscek *et al.* (1996a,b) calculated the hydrofracture shapes from the time-lapse temperature logs in seven observation wells. For calibration, they used the pilot geology, overall steam injection rates and pressures, and the analysis of Ilderton *et al.* (1996) detailing the azimuth and initial extent of the two hydrofractures.

Wright and Conant (1995), Wright *et al.* (1997) have used surface and downhole tiltmeters to map the orientation and sizes of vertical and horizontal hydrofractures. They observed fracture reorientation on dozens of staged fracture treatments in several fields, and related it to reservoir compaction caused by insufficient and nonuniform water injection. By improving the tiltmeter sensitivity, Wright *et al.* (1997) have been able to determine fracture azimuths and dips down to 3,000 m. Most importantly, they have used downhole tiltmeters in remote observation wells to determine hydrofracture dimensions, height, width and length. This approach might be used in time-lapse monitoring of hydrofracture growth.

Recently, Ovens *et al.* (1998) analyzed the growth of water injection hydrofractures in a low-permeability chalk field. Water injection above fracture propagation pressure is used there to improve oil recovery. Ovens *et al.*, have calculated fracture growth with Koning's (Koning, 1985) and Ovens-Niko (Ovens *et al.*, 1998) 1D models. Their conclusions are similar to those in this paper. Most notably, they report hydrofractures tripling in length in 800 days.

Numerous attempts have been undertaken to model fracture propagation both numerically and analytically. We just note the early fundamental papers (Zheltov and Khristianovich, 1955; Biot, 1956, 1972; Barenblatt, 1959a,b,c, 1961), and refer the reader to a monograph (Valko and Economides, 1995) for further references.

We do not attempt to characterize the geometry of the hydrofracture. In the mass balance equation presented below, the fracture area and the injection pressure and rate are most important. Because the hydrofracture width is much less than its two other dimensions and the characteristic width of the pressure propagation zone, we neglect it when we derive and solve the pressure diffusion equation. At the same

time, we assume a constant effective hydrofracture width when we account for the fracture volume in the fluid mass balance.

This paper is organized as follows. First, we present a 2D model of pressure diffusion from a growing fracture. We apply the self-similar solution of the transient pressure equation by Gordeyev and Entov (Gordeyev and Entov, 1997). This solution is obtained under the assumption of constant injection pressure. Using Duhamel's principle, see for example (Tikhonov and Samarskii, 1963), we generalize the Gordeyev and Entov solution to admit variable injection pressure, which of course is not self-similar. We use this solution to conclude that the flow of water injected into a low-permeability formation preserves its linear structure for a long time. Moreover, in the diatomite waterfloods, the flow is almost strictly linear because the distance between neighboring wells in a staggered line drive is about 45 m, and this is approximately equal to one half of the fracture length.

Therefore, we restrict our analysis to 1D linear flow, noting that in a higher permeability formation the initially linear flow may transform into a pseudo-radial one at a much earlier stage. In this context, we revisit Carter's theory (Howard and Fast, 1957) of fluid injection through a growing hydrofracture. Aside from the mass balance considerations, we incorporate variable injection pressure into our model. In particular, a new simple expression is obtained for the cumulative fluid injection as a function of the variable injection pressure and the hydrofracture area. Fracture growth is expressed in terms of readily available field measurements. The results are presented, we hope, in a clear and concise form.

2. Theory

2.1. PRESSURE FIELD IN 2D

Let us analyze pressure diffusion in 2D using the self-similar solution by Gordeyev and Entov (1997), obtained under the assumption of constant injection pressure. Since this solution as represented by Equations (2.5) and (3.4) in (Gordeyev and Entov, 1997) has a typo, we briefly overview the derivation and present the correct form (Equation (14) below). Using Duhamel's principle, we generalize this solution to admit time-dependent injection pressure.

The fluid flow is two-dimensional and it satisfies the well-known pressure diffusion equation (Muskat, 1946)

$$\frac{\partial p(t, x, y)}{\partial t} = \alpha_w \nabla^2 p(t, x, y), \tag{1}$$

where $p(t, x, y)$ is the pressure at point (x, y) of the reservoir at time t, α_w is the overall hydraulic diffusivity, and ∇^2 is the Laplace operator. The coefficient α_w combines both the formation and fluid properties, (Zwahlen and Patzek, 1997a).

In Equation (1) we have neglected the capillary pressure. As first implied by Rapoport and Leas (Rapoport and Leas, 1953), the following inequality determines when capillary pressure effects are important in a waterflood

$$\mathrm{N}_{RL} \equiv \sqrt{\frac{\phi}{k}} \frac{\mu u L}{k_{rw} \varphi \gamma_{ow} \cos\theta} < 3 \tag{2}$$

where u is the superficial velocity of water injection, and L is the macroscopic length of the system. In the low-permeability, porous diatomite, $k \approx 10^{-16}\,\mathrm{m}^2$, $\phi \approx 0.50$. $u \approx 10^{-7}\,\mathrm{m/s}$, $L \approx 10\,\mathrm{m}$, $k_{\mathrm{rw}} \approx 0.1$, $\gamma_{\mathrm{ow}} \cos\theta \approx 10^{-3}\,\mathrm{N/m}$, and $\mu \approx 0.5 \times 10^{-3}$ Pa-s. Hence the Rapoport–Leas number (Rapoport and Leas, 1953) for a typical waterflood in the diatomite is of the order of 100, a value that is much larger than the criterion given in Equation (2). Thus capillary pressure effects are not important for water injection at a field scale. Of course, capillary pressure dominates at the pore scale, determines the residual oil saturation to water, and the ultimate oil recovery. This, however, is a completely different story (see Patzek, 2000).

To impose the boundary conditions, consider a pressure diffusion process caused by water injection from a vertical rectangular hydrofracture totally penetrating a homogeneous, isotropic reservoir filled with a slightly compressible fluid of similar mobility. Assume that the fracture height does not grow with time. The fracture width is negligible in comparison with the other fracture dimensions and the characteristic length of pressure propagation, therefore we put it equal to zero.

Denote by $L(t)$ the half-length of the fracture. Place the injector well on the axis of the fracture and require the fracture to grow symmetrically with respect to its axis. Then, it is convenient to put the origin of the coordinate system at the center of the fracture, Figure 1.

The pressure inside the fracture is maintained by water injection and it may depend on time. Denote the pressure in the fracture by $p_0(t, y)$, $-L(t) \leqslant y \leqslant L(t)$. Then the boundary-value problem can be formulated as follows: find a function $p(t, x, y)$, which satisfies the differential Equation (1) for all (t, x, y), $t \geqslant 0$, and (x, y) outside the line segment $\{-L(t) \leqslant y \leqslant L(t), x = 0\}$, such that the following initial and boundary conditions are satisfied:

$$p(0, x, y) = 0, \tag{3}$$

$$p(t, 0, y)|_{-L(t) \leqslant y \leqslant L(t)} = p_0(t, y) \tag{4}$$

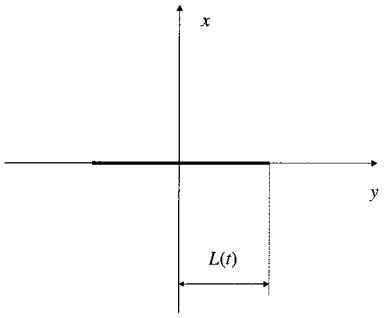

Figure 1. The coordinate system and the fracture.

and

$$p(t, x, y) \approx 0 \quad \text{for sufficiently large } r = \sqrt{x^2 + y^2}. \tag{5}$$

The conditions (3) and (5) mean that pressure is measured with respect to the initial reservoir pressure at the depth of the fracture. In the examples below, the low reservoir permeability implies that pressure remains at the initial level at distances of 30–60 m from the injection hydrofracture for 5–10 years.

To derive the general solution for pressure diffusion from a growing fracture, we rescale Equation (1) using the fracture half-length as the variable length scale:

$$x = L(t)\xi, \qquad y = L(t)\eta. \tag{6}$$

and $\tau = t$. In the new variables, Equation (1) takes on the form

$$L^2(\tau)\frac{\partial p(\tau, \xi, \eta)}{\partial \tau} = \alpha_w \nabla^2 p(\tau, \xi, \eta) + L(\tau)L'(\tau)\left(\xi\frac{\partial p(\tau, \xi, \eta)}{\partial \xi} + \eta\frac{\partial p(\tau, \xi, \eta)}{\partial \eta}\right). \tag{7}$$

Boundary condition (4) transforms into

$$p(\tau, \xi, \eta)|_{-1\leqslant\xi\leqslant 1} = p_0(\tau, \xi L(\tau)). \tag{8}$$

Initial condition (3) and boundary condition (5) transform straightforwardly.

In elliptic coordinates

$$\xi = \cosh\varphi\cos\theta, \qquad \eta = \sinh\varphi\sin\theta \tag{9}$$

Equation (7) and boundary conditions (8) and (5), respectively, transform into

$$4DL^2(\tau)\frac{\partial p(\tau, \varphi, \theta)}{\partial \tau} = 4\alpha_w \nabla^2 p(\tau, \varphi, \theta) + \frac{d}{\mathrm{d}\tau}(L(\tau)^2) \times \times \left(\sinh 2\varphi\frac{\partial p(\tau, \varphi, \theta)}{\partial \varphi} - \sin 2\theta\frac{\partial p(\tau, \varphi, \theta)}{\partial \theta}\right) \tag{10}$$

and

$$p(\tau, 0, \theta) = p_0(\tau, L(\tau)\cos\theta), \tag{11}$$

$$\lim_{\varphi\to\infty} p(\tau, \varphi, \theta) = 0. \tag{12}$$

Because the problem is symmetric, we can restrict our considerations to the domain $\{x \geqslant 0, y \geqslant 0\}$. The symmetry requires that there be no flow through the coordinate axes, that it imposes two additional Neumann boundary conditions:

$$\left.\frac{\partial p(t, \xi, \eta)}{\partial \xi}\right|_{\substack{\xi=0\\ \eta\geqslant 0}} = \left.\frac{\partial p(t, \xi, \eta)}{\partial \eta}\right|_{\substack{\xi>1\\ \eta=0}} = 0. \tag{13}$$

For constant injection pressure, $p_0(\tau, \theta) = p_0 = \text{const}$, and the square-root of time fracture growth, $L(t) = \sqrt{at}$, a self-similar solution can be obtained:

$$p(\tau, \varphi, \theta) = p_0 \left(1 - U_0 \int_0^{\varphi} \exp\left(\frac{-a\cosh(2\nu)}{8\alpha_w}\right) \mathrm{d}\nu\right), \tag{14}$$

where $U_0 = 2/K_0(k_\tau/2)$, $k_\tau = a/4\alpha_w$ and $K_0(\cdot)$ is the modified Bessel function of the second kind (Carslaw and Jaeger, 1959; Tikhonov and Samarskii, 1963). Note that Equations (2.5) and (3.4) in (Gordeyev and Entov, 1997) have one extra division by $\cosh(2\nu)$. This typo is fixed in Equation (14).

To obtain the solution with the time-dependent injection pressure, we need to express solution (14) in the original Cartesian coordinates. From (9)

$$\varphi(t, x, y) = \operatorname{arccosh}\left(\sqrt{\frac{at + x^2 + y^2 + \sqrt{(at + x^2 + y^2)^2 - 4aty^2}}{2at}}\right). \tag{15}$$

Now, the solution (14) can be extended to the case of time-dependent injection pressure by using Duhamel's principle (Tikhonov and Samarskii, 1963). For this purpose put

$$U(t, x, y) = 1 - U_0 \int_0^{\varphi(t,x,y)} \exp\left(\frac{-a\cosh(2\nu)}{8\alpha_w}\right) \mathrm{d}\nu. \tag{16}$$

Then for the boundary condition (4), with $p_0(t, y) = p_0(t)$, one obtains

$$p(t, x, y) = \int_0^t \frac{\partial U(t - \tau, x, y)}{\partial t} p_0(\tau)\, \mathrm{d}\tau. \tag{17}$$

The assumption of square-root growth rate $L(t) = \sqrt{at}$ reasonably models the fact that the growth has to slow down as the fracture increases. At the same time, it leads to a simple exact solution given in Equation (17). The fourth-root growth rate obtained in (Gordeyev and Zazovsky, 1992) behaves similarly at larger t, therefore, the square-root rate represents a qualitatively reasonable approximation. This growth rate model was used for the leakoff flow analysis in (Valko and Economides, 1995).

2.2. EXAMPLES

Here we present the results of several simulations of pressure diffusion in layer G of the South Belridge diatomite, see Table I and (Zwahlen and Patzek, 1997a). In the simulations, we have assumed that the pressure in the hydrofracture is hydrostatic and is maintained at 2.07×10^4 Pa (≈ 300 psi) above the initial formation pressure in layer G. The fracture continues to grow as the square root of time, and it grows up to 30 m tip-to-tip during the first year of injection. Figures 2–4 show the calculated pressure distributions after 1, 2, 5 and 10 years of injection in layer

Table I. South Belridge, Section 33, properties of diatomite layers

Layer	Thickness [m]	Depth [m]	Porosity	Permeability [md]	Diffusivity [m^2/Day]
G	62.8	223.4	0.57	0.15	0.0532
H	36.6	273.1	0.57	0.15	0.0125
I	48.8	315.2	0.54	0.12	0.0039
J	48.8	364.5	0.56	0.14	0.0395
K	12.8	395.3	0.57	0.16	0.0854
L	49.4	426.4	0.54	0.24	0.0396
M	42.7	472.4	0.51	0.85	0.0242

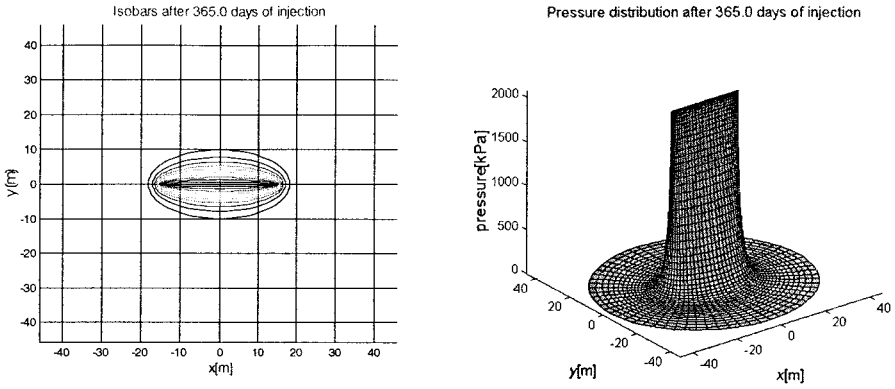

Figure 2. Relative pressure distribution after 1 year of injection.

G. For permeability and diffusivity we use more convenient units millidarcy [md] (1 md $\approx 9.869 \times 10^{-16}\,\mathrm{m}^2$) and m^2/Day ($86400\,\mathrm{m}^2/\mathrm{Day} = 1\,\mathrm{m}^2/\mathrm{s}$).

Note that even after 10 years of injection, the high-pressure region does not extend beyond 30 m from the fracture. The flow direction is orthogonal to the isobars. The oblong shapes of the isobars demonstrate that the flow is close to linear and it is almost perpendicular to the fracture even after a long time.

Figure 6 shows how the formation pressure builds up during 10 years of injection in the plane intersecting the fracture center (left) and intersecting its wing 30 m along the fracture (right). Comparison of the two plots in Figure 6 demonstrates that the injected water flow is remarkably parallel.

Another illustration is provided by Figure 7 and 8, where the formation pressure is plotted versus the distance from the fracture at 0, 15, 30 and 46 m away from the center. The pressure distribution is very close to parallel soon after the fracture length reaches the respective distance. For instance, in Figure 7 the pressure distribution at the cross-section 45 m away from the center is different because the

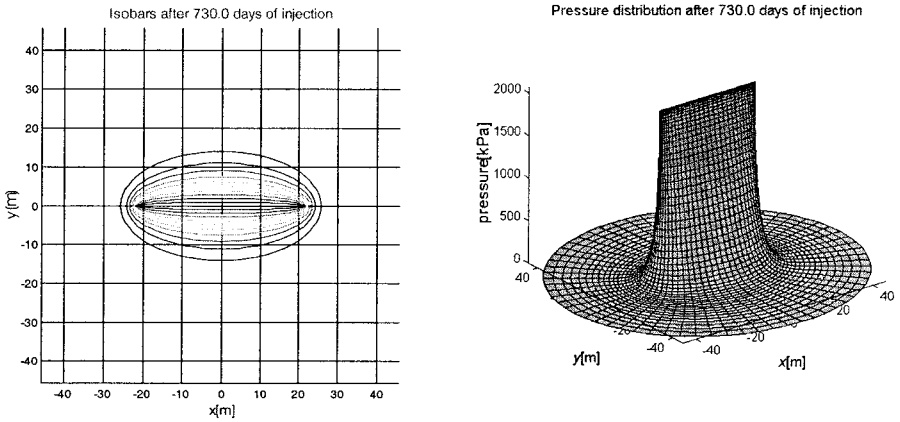

Figure 3. Relative pressure distribution after 2 years of injection.

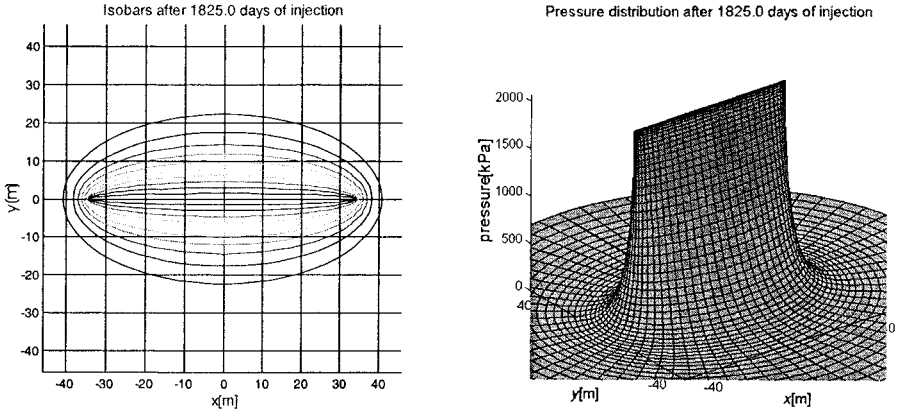

Figure 4. Relative pressure distribution after 5 years of injection.

fracture is not yet long enough. After 5 years, the pressure distribution becomes almost parallel at all distances from the center.

As we remarked earlier, diatomaceous reservoirs are layered and the layers are non communicating. The linearity of flow is observed in the different layers, Figure 9. Computations show that in each layer the pressure distribution after 5 years of injection is almost the same looking down on the center of the fracture and on its wing 30 m away from the center. Therefore, the injected water flow is essentially linear. This observation allows us to cast our water injection model as one-dimensional. In the following section, we incorporate the variable injection pressure into Carter's model and obtain an elegant equation expressing the cumulative fluid injection through the injection pressure and the fracture size.

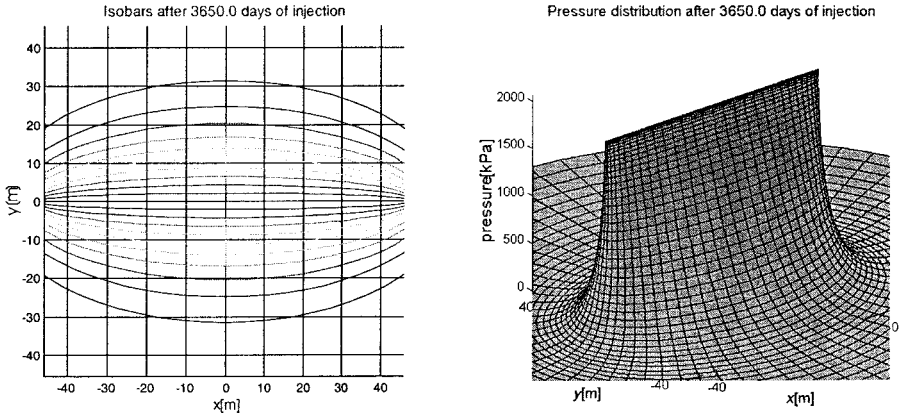

Figure 5. Relative pressure distribution after 10 years of injection. Note the change of scale in the isobar contour plot in comparison with Figure 4.

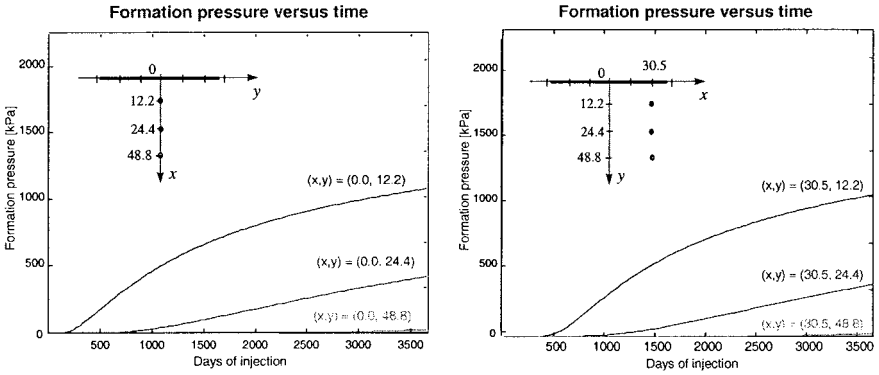

Figure 6. Pressure histories at three fixed points, 12, 24 and 49 m away from the fracture, looking down on fracture center (left) and fracture wing 30 m along the fracture (right).

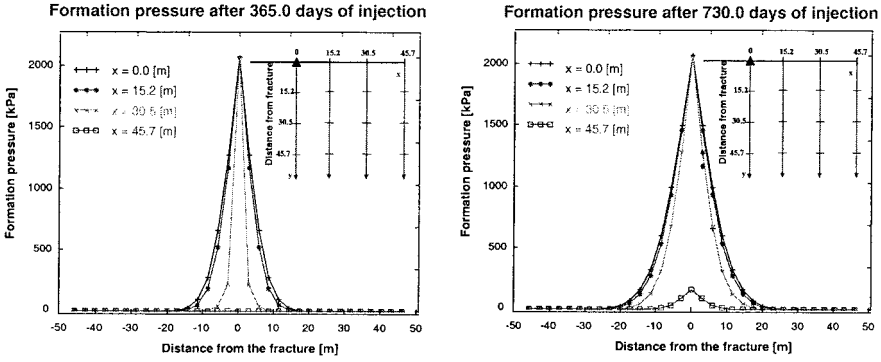

Figure 7. Pressure distributions along four cross-sections orthogonal to the fracture after 1 and 2 years of injection.

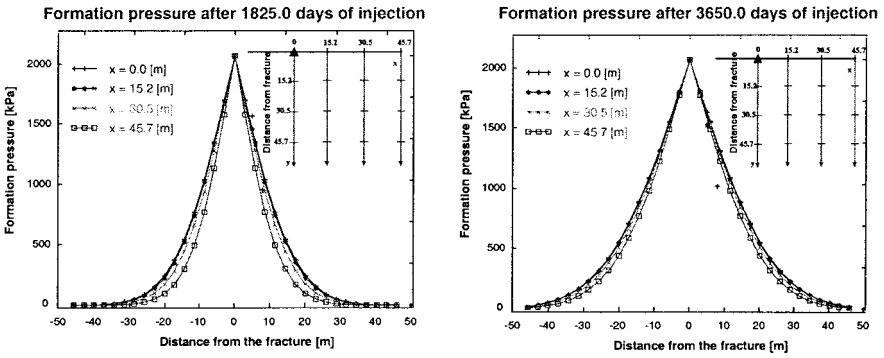

Figure 8. Pressure distributions in the same cross-sections after 5 and 10 years of injection.

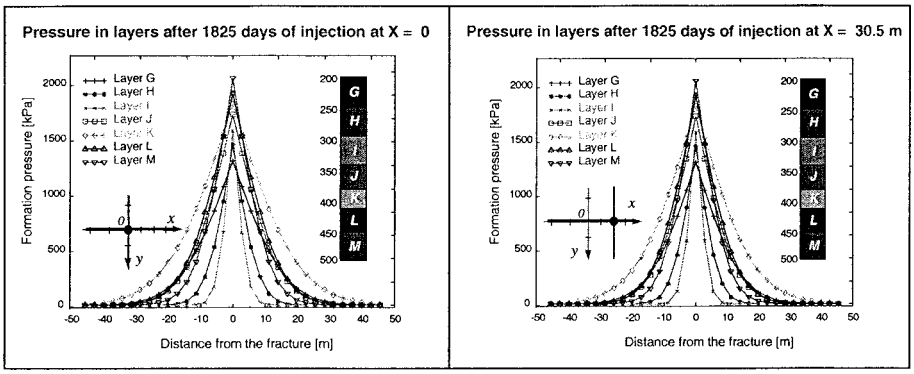

Figure 9. Pressure distributions in the diatomite layers after 5 years of injection. The cross-sections at 0 and 30.5 m from the center of the fracture are shown.

2.3. CARTER'S MODEL REVISITED

Here, we proceed to formulate a one-dimensional model of isothermal fluid injection from a vertical highly conductive fracture that fully penetrates a low-permeability reservoir. We neglect the compressibility of the injected fluid and assume that the flow is horizontal, transient, and perpendicular to the fracture plane. It is important that the hydrofracture may grow during the injection. We denote by $A(t)$ and $\mathrm{d}A(t)/\mathrm{d}t$ the fracture area and the rate of fracture growth at time t, respectively. We start counting time right after completion of the fracturing job, so $A(0)$ is not necessary equal to zero. We denote by $q(t)$ and $p_{\mathrm{inj}}(t)$ the injection rate and the average downhole injection pressure, respectively. We assume that the fluid pressure is essentially the same throughout the fracture at each time.

Let us fix a current time t and pick an arbitrary time τ between 0 and t. As the fracture is growing, different parts of it become active at different times. We define $u_\tau(t)$ as the fluid superficial leak-off velocity at time t across that portion of

the fracture, which opened between τ and $\tau + \Delta\tau$, where $\Delta\tau$ is a small increment of time. The area of the part of the fracture, which has been created in the time interval $[\tau, \tau + \Delta\tau]$, is equal to $A(\tau + \Delta\tau) - A(\tau)$. Hence, the rate of fluid leak-off through this area is equal to $\Delta q_\tau(t) \approx 2u_\tau(t)(A(\tau + \Delta\tau) - A(\tau))$. The coefficient of 2 is implied by the assumption that the fracture is two-sided and the fluid leaks symmetrically into the formation. The rate of leak-off from the originally open fracture area is $q_0(t) = 2u_0(t)A(0)$. Let us split the time interval $[0, t]$ by a partition $\{0 = \tau_0 < \tau_1 < \cdots < \tau_K = t\}$ into small contiguous non-overlapping subintervals $[\tau_k, \tau_k + \Delta\tau_k]$, $\Delta\tau_k = \tau_{k+1} - \tau_k$, and apply the above calculations to each subinterval. Summing up over all intervals $[\tau_k, \tau_k + \Delta\tau_k]$ and adding the rate of water accumulation inside the fracture $V(t)/\mathrm{d}t$, one gets:

$$\begin{aligned} q(t) \approx\ & 2u_0(t)A(0) + 2u_{\tau_0}(t)(A(\tau_0 + \Delta\tau_0) - A(\tau_0)) + \\ & + 2u_{\tau_1}(t)(A(\tau_1 + \Delta\tau_1) - A(\tau_1)) + \cdots + 2u_{\tau_{K-1}}(t) \times \\ & \times (A(\tau_{K-1} + \Delta\tau_{K-1}) - A(\tau_{K-1})) + \frac{\mathrm{d}V}{\mathrm{d}t}. \end{aligned} \tag{18}$$

Here $V(t)$ is the volume of the fracture at time t. It is convenient for further calculations to introduce an effective or average fracture width w: $w = V(t)/A(t)$. We assume that w is constant. Passing to the limit as $\max_k(\Delta\tau_k) \to 0$, we obtain

$$q(t) = 2u_0(t)A(0) + 2\int_0^t u_\tau(t)\frac{\mathrm{d}A(\tau)}{\mathrm{d}\tau}\,\mathrm{d}\tau + w\frac{\mathrm{d}A(t)}{\mathrm{d}t}. \tag{19}$$

Equation (19) extends the original Carter's model (Howard and Fast, 1957) of fracture growth by accounting for the initial fracture area $A(0)$ and admitting a general dependence of the leak-off velocity on t and τ (in original Crater's model $u_\tau(t) = u(t - \tau)$).

In order to incorporate the variable injection pressure into Equation (19), we need to find out how $u_\tau(t)$ depends on $p_{\mathrm{inj}}(t)$. From Darcy's law

$$u_\tau(t) = -\frac{kk_{\mathrm{rw}}}{\mu}\frac{\partial p_\tau(0, t)}{\partial x}. \tag{20}$$

Here k and k_{rw} are the absolute rock permeability and the relative water permeability in the formation outside the fracture, and μ is the water viscosity. $\partial p_\tau(0, t)/\partial x$ is the pressure gradient on the fracture face along the part of the fracture that opened at time τ, and $p_\tau(x, t)$ is the solution to the following boundary-value problem:

$$\begin{aligned} & \frac{\partial p_\tau}{\partial t} = \alpha_w\frac{\partial^2 p_\tau}{\partial x^2}, \qquad t \geqslant \tau, \qquad x \geqslant 0, \\ & p_\tau(x, \tau) = \begin{cases} p_{\mathrm{inj}}(\tau), & x = 0, \\ p_i, & x > 0, \end{cases} \qquad p_\tau(0, t) = p_{\mathrm{inj}}(t). \end{aligned} \tag{21}$$

Here α_w and p_i denote, respectively, the hydraulic diffusivity and the initial formation pressure. The solution to the boundary-value problem (21) characterizes the distribution of pressure outside the fracture caused by fluid injection. Hence, $p_\tau(x,t)$ is the pressure at time t at a point located at distance x from a portion of the fracture that opened at time τ. Solving the boundary value problem (21), we obtain that

$$\left.\frac{\partial p_\tau(x,t)}{\partial x}\right|_{x=+0} = -\left(\frac{1}{\sqrt{\pi\alpha_w(t-\tau)}}[p_{\text{inj}}(\tau)-p_i]+\frac{1}{\sqrt{\pi\alpha_w}}\int_\tau^t \frac{p'_{\text{inj}}(\xi)}{\sqrt{t-\xi}}\,\mathrm{d}\xi\right), \tag{22}$$

where the prime denotes derivative. Substitution into (20) yields

$$u_\tau(t) = \frac{kk_r}{\mu}\left(\frac{1}{\sqrt{\pi\alpha_w(t-\tau)}}[p_{\text{inj}}(\tau)-p_i]+\frac{1}{\sqrt{\pi\alpha_w}}\int_\tau^t \frac{p'_{\text{inj}}(\xi)}{\sqrt{t-\xi}}\,\mathrm{d}\xi\right). \tag{23}$$

Combining Equations (23) and (19), we obtain

$$\begin{aligned} q(t) \;=\; & w\frac{\mathrm{d}A(t)}{\mathrm{d}t} + \\ & + 2\frac{kk_{\text{rw}}}{\mu\sqrt{\pi\alpha_w}}(p_{\text{inj}}(0)-p_i)\left(\frac{A(0)}{\sqrt{t}}+\int_0^t \frac{1}{\sqrt{t-\xi}}\frac{\mathrm{d}A(\xi)}{\mathrm{d}\xi}\,\mathrm{d}\xi\right) + \\ & + 2\frac{kk_{\text{rw}}}{\mu\sqrt{\pi\alpha_w}}\int_0^t p'_{\text{inj}}(\tau)\left(\frac{A(\tau)}{\sqrt{t-\tau}}+\int_\tau^t \frac{1}{\sqrt{t-\xi}}\frac{\mathrm{d}A(\xi)}{\mathrm{d}\xi}\,\mathrm{d}\xi\right)\mathrm{d}\tau. \end{aligned} \tag{24}$$

Further calculations imply that Equation (24) can be recast into the following equivalent form:

$$Q(t) = wA(t) + 2\frac{kk_{\text{rw}}}{\mu\sqrt{\pi\alpha_w}}\int_0^t \frac{(p_{\text{inj}}(\tau)-p_i)A(\tau)}{\sqrt{t-\tau}}\,\mathrm{d}\tau \tag{25}$$

where $Q(t) = wA(0) + \int_0^t q(\tau)\,\mathrm{d}\tau$ is the cumulative injection at time t.

Equation (24) states the following. Current injection rate cannot be determined solely from the current fracture area and the current injection pressure; instead, it depends on the entire history of injection. The convolution with $1/\sqrt{t-\tau}$ implies that recent history is the most important factor affecting the current injection rate. The last conclusion is natural. Since the fracture extends into the formation at the initial pressure, the pressure gradient is greater on the recently opened portions of the fracture.

Our model allows us to calculate analytically the pressure gradient (22) and the leak-off velocity at the boundary. Therefore, we avoid errors from numerical differentiation of the pressure distribution at the fracture face where the gradient takes on its largest value.

3. Discussion

Equation(25) encompasses the following special cases:

(1) If there is no fracture growth and injection pressure is constant, that is, $A(t) \equiv A_0$ and $p_{\text{inj}}(t) \equiv p_{\text{inj}}$, then

$$Q(t) = wA_0 + 4A_0 \frac{kk_{\text{rw}}}{\mu\sqrt{\pi\alpha_w}}(p_{\text{inj}} - p_i)\sqrt{t} \tag{26}$$

and injection rate must decrease inversely proportionally to the square root of time

$$q(t) = 2\frac{kk_{\text{rw}}}{\mu\sqrt{\pi\alpha_w}}(p_{\text{inj}} - p_i)\frac{A_0}{\sqrt{t}}. \tag{27}$$

The leak-off velocity is

$$u(t) \;=\; \frac{q(t)}{2A_0} = \frac{kk_{\text{rw}}}{\mu}\frac{(p_{\text{inj}} - p_i)}{\sqrt{\pi\alpha_w t}} = \frac{C}{\sqrt{t}}, \quad \text{where} \quad C = \frac{kk_{\text{rw}}}{\mu}\frac{(p_{\text{inj}} - p_i)}{\sqrt{\pi\alpha_w}}. \tag{28}$$

The coefficient C is often called leakoff coefficient, see for example (Kuo *et al.*, 1984) The cumulative fluid injection can be expressed through C

$$\begin{aligned} Q(t) \;&=\; wA_0 + 4A_0\frac{kk_{\text{rw}}}{\mu}\frac{(p_{\text{inj}} - p_i)}{\sqrt{\pi\alpha_w}}\sqrt{t} = wA_0 + 4A_0C\sqrt{t} \\ &=\; wA_0 + (\text{Early Injection slope})\sqrt{t}, \end{aligned} \tag{29}$$

where the 'Early Injection Slope' characterizes fluid injection prior to fracture growth and prior to changes in injection pressure.

Equation (27) provides another proof of inevitability of fracture growth. The only way to prevent it at constant injection pressure is to decrease the injection rate according to $1/\sqrt{t}$. This strategy did not work in the field (Patzek, 1992).

(2) If there is no fracture growth, but injection pressure depends on time, then the cumulative injection is

$$Q(t) = wA_0 + 2A_0\frac{kk_{\text{rw}}}{\mu\sqrt{\pi\alpha_w}}\int_0^t \frac{(p_{\text{inj}}(\tau) - p_i)}{\sqrt{t-\tau}}\,\mathrm{d}\tau. \tag{30}$$

If injection pressure is bounded, $p_{\text{inj}}(t) \leqslant P_0$, then

$$Q(t) \leqslant wA_0 + 2A_0\frac{kk_{\text{rw}}}{\mu\sqrt{\pi\alpha_w}}(P_0 - p_i)\sqrt{t}. \tag{31}$$

Consequently, injection rate cannot satisfy $q(t) \geqslant q_0 > 0$ for all t, because otherwise one would have $Q(t) \geqslant wA_0 + q_0 t$, that contradicts Equation (31) for

$$t > 4\frac{A_0^2(P_0 - p_i)^2}{q_0^2}\frac{k^2k_{\text{rw}}^2}{\mu^2\pi\alpha_w}. \tag{32}$$

The expression on right-hand side of Equation (32) estimates the longest elapsed time of fluid injection at a rate greater than or equal to q_0, without fracture extension and without exceeding the maximum injection pressure. For the South Belridge diatomite (Patzek, 1992; Zwahlen and Patzek, 1997b), Equation (32) implies that this time is 100–400 days for $q_0 = 7950$ l/Day per fracture at a depth of 305 m. Maintaining high injection rate requires an increase of the downwhole pressure that makes fracture growth inevitable, regardless of the design of injection wells and injection policy.

(3) At constant injection pressure, both the cumulative injection and the injection rate are completely determined by the fracture growth rate

$$Q(t) = wA(t) + 2\frac{kk_{\mathrm{rw}}}{\mu\sqrt{\pi\alpha_w}}(p_{\mathrm{inj}} - p_i)\int_0^t \frac{A(\tau)}{\sqrt{t-\tau}}\,\mathrm{d}\tau, \tag{33}$$

$$q(t) = w\frac{\mathrm{d}A(t)}{\mathrm{d}t} + 2\frac{kk_{\mathrm{rw}}}{\mu\sqrt{\pi\alpha_w}}(p_{\mathrm{inj}} - p_i)\left(\frac{A(0)}{\sqrt{t}} + \int_0^t \frac{1}{\sqrt{t-\xi}}\frac{\mathrm{d}A(\xi)}{\mathrm{d}\xi}\,\mathrm{d}\xi\right). \tag{34}$$

This means that if the fracture stops growing at a certain moment, the injection rate must decrease inversely proportionally to the square root of time. Perhaps the most favorable situation would be obtained if the fracture grew slowly and continuously and supported the desired injection rate at a constant pressure. However, since the fracture growth is beyond our control, such an ideal situation is hardly attainable.

(4) If the cumulative injection and injection rate are, respectively, equal to

$$Q(t) = wA_0 + 4\frac{kk_{\mathrm{rw}}}{\mu\sqrt{\pi\alpha_w}}(p_{\mathrm{inj}} - p_i)A_0\sqrt{t} + q_0 t \tag{35}$$

and

$$q(t) = 2\frac{kk_{\mathrm{rw}}}{\mu\sqrt{\pi\alpha_w}\sqrt{t}}(p_{\mathrm{inj}} - p_i)A_0 + q_0, \tag{36}$$

then the solution to Equation (34) with respect to $A(t)$ is provided by

$$A(t) = A_0 + \frac{q_0 w}{4\pi C^2}\left[e^{\tau_D}\mathrm{erfc}(\sqrt{\tau_D}) + \frac{2}{\sqrt{\pi}}\sqrt{\tau_D} - 1\right], \tag{37}$$

where

$$\tau_D = \frac{4\pi C^2}{w^2}t = \frac{\pi}{4}\left(\frac{\text{Early Injection Slope}}{\text{Initial Fracture Volume}}\right)^2 t \tag{38}$$

is the dimensionless drainage time of the initial fracture, and wA_0 is the 'spurt loss' from the instantaneous creation of fracture at $t = 0$ and filling it with fluid. Formula (36) for the injection rate consists of two parts: the first component is the leak-off

rate when there is no fracture extension and the second, constant, component is 'spent' on the fracture growth. Conversely, the first constant term in the solution (37) is produced by the first term in (36) and the second additive term is produced by the constant component q_0 of $q(t)$ in (36). In particular, if $A_0 = 0$, we recover Carter's solution (see Equation (A5), (Howard and Fast, 1957)).

If $q(t) \approx q_0$ for longer injection times, then

$$A(t) \approx A_0 \left(1 + \frac{q_0}{\pi C A_0}\sqrt{t}\right) = A_0 \left(1 + \frac{4q_0}{\pi \text{ Early Injection Slope}}\sqrt{t}\right), \quad (39)$$

where the average fluid injection rate q_0 and the Early Injection Slope are in consistent units. For short injection times, the hydrofracture area may grow linearly with time, see for example, (Valko and Economides, 1995), page 174.

Equation (39) allows one to calculate the fracture area as a function of the average injection rate and the early slope of cumulative injection versus the square root of time. All of these parameters are readily available if one operates a new injection well for a while at a low and constant injection pressure to prevent fracture extension. The initial fracture area (i.e., its length and height) is known approximately from the design of the hydrofracturing job (Wright and Conant, 1995, Wright *et al.*, 1997). In Part 2, we show how our model can be used to estimate the hydrofracture size from the injection pressure-rate data.

The most important restriction in Carter's and our derivation is the requirement that the injection pressure is not communicated beyond the current length of the fracture. Hagoort *et al.* (1980) have shown numerically that for a homogeneous reservoir the fracture propagation rate is only about half of that predicted by the Carter formula (Equation (37) with $A_0 = 0$). This is because the formation pressure increases beyond the current length of the hydrofracture, thus confining it. If fracture growth is slower than predicted by the mass balance (39), then there must be flow parallel to the fracture plane or additional formation fracturing perpendicular to the fracture plane, or both. Either way, the leak-off rate from the fracture must increase.

In Part II of this paper, we address the issue of injection control subject to the fracture growth.

4. Conclusions

1. We have analyzed 2D, transient water injection from a growing vertical hydrofracture. The application of the self-similar solution by Gordeyev and Entov (1997) to a low-permeability rock leads us to conclude that the water flow is approximately orthogonal to the fracture plane for a long time.
2. We have revised Carter's transient mass balance of fluid injection through a growing fracture and complemented the mass balance equation with effects of variable injection pressure. The extended Carter formula has been presented in a new simplified form.

3. We have proved that the rate of fluid injection through a static hydrofracture must fall down to almost zero if injection pressure is bounded by, say, the overburden stress.
4. Thus, ultimately, fracture growth is inevitable regardless of mechanical design of injection wells and injection policy. However, better control of injection pressure through improved mechanical design is always helpful.
5. In diatomite, fracture extension must occur no later than 100–400 days for water injection rates of no less than 8000 l/Day per fracture and downhole injection pressure increasing up to the fracture propagation stress.
6. In 20 fluid injection wells in three different locations in the Belridge diatomite, in some 40 water injectors in the Lost Hills diatomite, and in several water injectors in the Dan field, the respective hydrofractures underwent continuous extension with occasional, discrete failures. Therefore, as we have predicted, extensions of injection hydrofractures are a norm in low-permeability rock.
7. These hydrofracture extensions manifested themselves as constant injection rates at constant injection pressures. The magnitude of hydrofracture extension can be estimated over a period of 4–7 years from the initial slope of the cumulative injection versus the square root of time, average injection rate, and by assuming a homogeneous reservoir. In the diatomite, the hydrofracture areas may extend by a factor of 2.5–5.5 after 7 years of water or steam injection. In the Dan field, the rate of growth is purposefully higher, a factor of 2–3 in 3 years of water injection.

Acknowledgements

The authors are thankful to the reviewers for their valuable remarks. This work was supported in part by two members of the U.C. Oil® Consortium, Chevron Petroleum Technology Company, and CalResources (now Aera Energy), LLC. Partial support was also provided by the Assistant Secretary for Fossil Energy, Office of Gas and Petroleum Technology, under contract No. DE-ACO3-76FS00098 to the Lawrence Berkeley National Laboratory of the University of California. We thank CalResources for releasing the Phase II steam pilot data, and Crutcher-Tufts for releasing the Dow-Chanslor waterflood data. We also thank Mobil E&P US for providing the Lost Hills I waterflood data.

References

Barenblatt, G. I.: 1959a, Concerning equilibrium cracks forming during brittle fracture. The stability of isolated cracks. Relationships with energetic theories, *J. Appl. Math. Mech.* **23**(5), 1273–1282.

Barenblatt, G. I.: 1959b, Equilibrium cracks formed during brittle fracture. rectilinear cracks in plane plates. *J. Appl. Math. Mech.* **23**(4), 1009–1029.

Barenblatt, G. I.: 1959c, The Formation of equilibrium cracks during brittle fracture. General ideas and hypotheses. Axially-symmetric cracks, *J. Appl. Math. Mech.* **23**(3), 622–636.

Barenblatt, G. I.: 1961, On the finiteness of stresses at the leading edge of an arbitrary crack, *J. Appl. Math. Mech.* **25**(4), 1112–1115.

Biot, M. A.: 1956, Theory of deformation of a porous viscoplastic anisotropic solid, *J. Appl. Phys.* **27**, 459–467.

Biot, M. A.: 1972, Mechanics of finite deformation of porous solids, *Indiana Uni. Math. J.* **21**, 597–620.

Carslaw, J. C. and Jaeger, J. C.: 1959, Conduction of Heat in Solids, 2nd edn, Clarendon Press, Oxford.

De, A. and Patzek, T. W.: 1999, Waterflood Analyzer, MatLab Software Package, Version, Lawrence Berkley National Lab, Berkeley, CA.

Gordeyev, Y. N. and Entov, V. M.: 1997, The pressure distribution around a growing crack, *J. Appl. Maths. Mechs.* **51**(6), 1025–1029.

Gordeyev, Y. N. and Zazovsky, A. F.: 1992, Self-similar solution for deep-penetrating hydraulic fracture propagation, *Transport in Porous Media* **7**, 283–304.

Hagoort, J., Weatherill, B. D. and Settari, A.: 1980, Modeling the propagation of waterflood-induced hydraulic fractures, *SPEJ* **8**, 293–303.

Howard, G. C. and Fast, C. R.: 1957, Optimum fluid characteristics for fracture extension, *Drill. Prod. Prac. API* 261–270.

Ilderton, D., Patzek, T. E. et al.: 1996, Microseismic imaging of hydrofractures in the diatomite, *SPE Form. Eval.* **3**, 46–54.

Koning, E. J. L.: 1985, Fractured water injection wells – analytical modeling of fracture propagation, *SPE* **14684**, 1–27.

Kovscek, A. R., Johnston, R. M. and Patzek, T. W.: 1996a, Interpretation of hydrofracture geometry– During steam injection using temperature transients, I. Asymmetric hydrofractures, *In Situ* **20**(3), 251–289.

Kovscek, A. R., Johnston, R. M. and Patzek, T. W.: 1996b, Interpretation of hydrofracture geometry during steam injection using temperature transients, II. Asymmetric hydrofractures, *In Situ* **20**(3), 289–309.

Kuo, M. C. T., Hanson, H. G. and DesBrisay, C. L.: 1984, Prediction of fracture extension during waterflood, *Paper SPE* **12769**, (Long Beach, (SPE)), 377–385.

Muskat, M.: 1946, The Flow of Homogeneous Fluids through Porous Media, J. W. Edwards, Ann Arbor, MI.

Ovens, J. E. V., Larsen, F. P. and Cowie, D. R.: 1998, Making sense of water injection fractures in the Dan field, *SPE Reser. Eval. Engng* **1**(6), 556–566.

Patzek, T. W.: 1992, Surveillance of South Belridge Diatomite, *SPE Western Regional Meeting* Paper SPE 24040, SPE, Bakersfield.

Patzek, T. W.: 2000, Verification of a complete pore network model of drainage and imbibition, *Twelfth SPE/DOE Symposium on Improved Oil Recovery*, SPE Paper 59312, Tulsa, SPE, OK; SPEJ, July 2001.

Patzek, T. W. and Silin, D. B.: 1998, Fluid injection into a low-permeability rock – 1. Hydrofrature growth, *SPE/DOE Eleventh Symposium on Improved Oil Recovery*, SPE, Tulsa, Oklahoma.

Rapoport, L. A. and Leas, W. J.: 1953, Properties of linear waterfloods, *Trans. AIME* **216**, 139–148.

Tikhonov, A. N. and Samarskii, A. A.: 1963, Equations of Mathematical Physics. International Series of Monographs in Pure and Applied Mathematics, Vol 39, Macmillan, New York.

Valko, P. and Economides, M. J.: 1995, Hydraulic Fracture Mechanics, Wiley, New York.

Vinegar, H. J. et al.: 1995, Active and passive seismic imaging of a hydraulic fracture in the diatomite, J. Petrol. Tech., **44**, 28.

Warpinski, N. R.: 1996, Hydraulic fracture diagnostics, *J. Petrol. Tech.* **10**.

Wright, C. A. and Conant, R. A.: 1995, Hydraulic fracture reorientation in primary and secondary recovery from low-permeability reservoirs, *SPE Annual Technical Conference & Exhibition*, SPE 30484, Dallas, TX.

Wright, C. A., Davis, E. J. et al.: 1997, Horizontal hydraulic fractures: Oddball occurrances or practical engineering concern? *SPE Western Regional Meeting*, SPE 38324, Long Beach, CA.

Zheltov, Y. P. and Khristianovich, S. A.: 1955, On hydraulic fracturing of an oil-bearing stratum, *Izv. Akad. Nauk SSSR. Otdel Tekhn. Nuk* **5**, 3–41.

Zwahlen, E. D. and Patzek, T. W.: 1997a, Linear transient flow solution for primary oil recovery with infill and conversion to water injection, *In Situ* **21**(4), 297–331.

Zwahlen, E. D. and Patzek, T. W.: 1997b, Linear transient flow solution for primary oil recovery with infill and conversion to water injection, *1997 SPE Western Regional Meeting*, SPE 38280, SPE, Long Beach.